

# Cold matter trapping via rotating helical optical potential.

A.Yu.Okulov\*

General Physics Institute of Russian Academy of Sciences Vavilova str. 38, 119991, Moscow, Russia

(Dated: May 17, 2010)

We consider a cold bosonic ensemble trapped by a helical interference pattern in the optical *loop* scheme. The counter propagating Laguerre-Gaussian beams with slightly detuned frequencies produce rotating helical potential provided their optical angular momenta are counter directed. The small frequency difference required for helix rotation might be induced by Sagnac effect. For the large number of atoms trapped by a slowly rotating helical optical potential the Gross-Pitaevskii equation is solved in Thomas-Fermi approximation. Two possible configurations of the atomic ensemble wavefunction are presented. The requirements for implementation of the optical *loop* scheme are briefly formulated.

PACS numbers: 37.10.Gh 42.50.Tx 67.85.Hj 42.65.Hw

## I. INTRODUCTION

Cold atoms trapping by the optical intensity gratings  $I(z, t) \sim \cos(\delta\omega t - 2k_z z)$  [1], where  $\delta\omega = c \cdot (k_f - k_b)$  is a frequency difference of the counter-propagating paraxial laser beams with the opposite wavevectors  $|\vec{k}_{f,b}| \approx k_z$ , have attracted a substantial attention from the point of view of quantum interference phenomena [2]. The interacting bosons in accelerated optical gratings with  $\delta\omega = \delta\omega \cdot t$  demonstrate Bloch oscillations, Landau-Zener tunneling in the non inertial reference frames [3]. The static optical lattices proved to be efficient as a many-body phenomena simulators [4, 5]. For example the trimerized optical **2D** kagomé lattices were used to study a low-temperature properties of fermion gases [6]. The rotating triangular and square optical lattices are capable to pin the vortices of cold boson at the antinodes (under *blue* detuning) of the optical interference pattern [7]. In addition to the **1D** and **2D** sinusoidal potential gratings, the optical vortices like LG beams offer a possibility to study persistent condensate flows in toroidal geometry [8]. In contrast to optical speckle patterns [9, 10], the isolated optical vortices (LG beams) are rectilinear in free space, the same holds for the phase-locked optical vortex arrays, observed in near-field of the *cw* solid-state microchip lasers [11–13]. These arrays of optical phase singularities might be used to demonstrate macroscopic BEC quantum state in the form of square array of the counter-rotating vortices pinned under *red* detuning at the nodes of the *nonrotating* interference pattern [14].

The standing wave interference patterns of the isolated counter propagating LG-beams had been demonstrated for the single atom trapping and detection [15]. As is shown in Sec. II following to [16] the phase-conjugation of the backward reflected LG transforms the **1D** sinusoidal intensity grating into the truly **3D** helicoidal pattern  $I(z, r, \theta, t)$  [17]. The key point in achieving this field

configuration (Sec.III) is in the opposite orbital angular momenta (OAM) of the interfering LG beams [18, 19]. We outline the purely *linear* optical setup for producing the helical interference patterns using phase conjugated LG-beams. The frequency splitting of the order of  $\delta\nu \cong 10^{-2} Hz$  of the counter propagating LG's in a typical table top *loop* setup might appear because of Sagnac effect due to the Earth rotation which have angular frequency  $\Omega_{\oplus} = 2\pi/86400$  [21]. The appearing laser frequency shift of the order  $\delta\omega = 2\pi\delta\nu$  leads to the rotation of the helical interference pattern around the propagation axis [16]. The question is whether the cold atomic ensemble will remain in the irrotational state or suddenly switched helical optical potential will impose to the atomic cloud the helical density profile and rotation.

In a present work we describe the possible regimes of condensate trapping by a slowly rotating helical potential. Two exact solutions of the Gross-Pitaevskii equation [20] for the mean field  $\Psi$  are obtained via Thomas-Fermi approximation (TFA) in Sec.IV. One solution has atomic density  $\rho_{helix}$  perfectly collocated with rotating optical helix  $I(z, r, \theta, t)$ , the other solution has nonrotating density  $\rho_{fun}$  profile with time-dependent phase.

## II. HELICAL INTERFERENCE PATTERN

It is well known that interference of a two counter-propagating optical waves with a slightly different frequencies  $\omega_f, \omega_b$  produces a running sinusoidal intensity grating [2, 22]. For the equal wave amplitudes  $|\mathbf{E}_f|, |\mathbf{E}_b|$  and the phase difference  $\phi$  the distribution of the light intensity  $I(z, r, \theta, t)$  have the following form in cylindrical coordinates  $z, r, \theta, t$  collocated with a propagation axis  $z$ :

$$\begin{aligned} I(z, r, \theta, t) &= |\mathbf{E}_f(z, r, \theta, t) + \mathbf{E}_b(z, r, \theta, t)|^2 \\ &\cong 2|\mathbf{E}_{(f,b)}|^2 [1 + \cos[(\omega_f - \omega_b)t - (k_f + k_b)z + \phi]], \end{aligned} \quad (1)$$

where a self-similar variable  $\chi = (\omega_f - \omega_b)t - (k_f + k_b)z + \phi$  is responsible for the translation of the interference pattern along  $z$  axis with the *group* velocity  $V_z = (\omega_f -$

\*Electronic address: alexey.okulov@gmail.com;  
URL: <http://www.gpi.ru/~okulov>

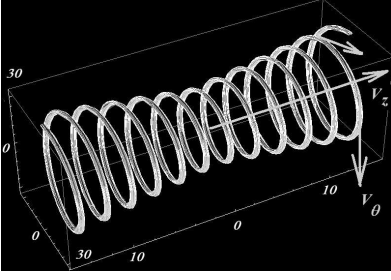


FIG. 1: The isosurface of the optical intensity  $I_{tw}$  and the Thomas-Fermi density  $\rho_{tw}$  of the cold atomic cloud in a helical optical dipole trap (6,23) (only one helix is shown for better visibility, the scale is in  $\mu m$ ). The spatial modulation of light intensity  $\cos(\delta\omega + 2kz \pm 2\ell\theta)$  (see equation (6)) is induced by the interference of counter-propagating LG waves with the opposite angular momenta. The pattern rotates with angular frequency  $\delta\omega$  as a "solid-body". This means that azimuthal speed of rotation is  $V_\theta = \delta\omega \cdot R$  while the axial speed, responsible for the helix pitch is equal to the group velocity of an overlapping LG's  $V_z = (\omega_f - \omega_b)/(k_f + k_b)$ . The isodensity surface  $\rho_{tw}$  of the helical atomic cloud rotates synchronously with the optical interference pattern.

$\omega_b)/(k_f + k_b)$ . Taking into account the transversal (in the plane  $(r, \theta)$ ) confinement of the light amplitudes  $\mathbf{E}_f, \mathbf{E}_b$  typical e.g. for a zeroth-order Gaussian beams :

$$\mathbf{E}_{(f,b)}(z, r, \theta, t) \approx |\mathbf{E}_{(f,b)}| \exp[-i\omega_{(f,b)}t \pm ik_{(f,b)}z] \exp\left[-\frac{r^2}{D_0^2(1 + iz/(k_{(f,b)}D_0^2))}\right], \quad (2)$$

where  $D_0$  - is a beam waist diameter, we see that the *roll* interference pattern (1) transforms into the sequence of equidistantly spaced rotationally invariant (in  $\theta$ ) *ellipsoids* picked up by propagation axis  $z$  [16]:

$$I(z, r, \theta, t) = |\mathbf{E}(z, r, \theta, t)|^2 = |\mathbf{E}_f(z, r, \theta, t) + \mathbf{E}_b(z, r, \theta, t)|^2 \cong 2|\mathbf{E}_{(f,b)}|^2 [1 + \cos[(\omega_f - \omega_b)t - (k_f + k_b)z]] \exp\left[-\frac{2r^2}{D_0^2(1 + z^2/(k_{(f,b)}^2 D_0^4))}\right], \quad (3)$$

provided that a visibility of pattern is good enough  $|\mathbf{E}_{(f)}| \cong |\mathbf{E}_{(b)}|$ .

For the higher-order propagation modes say Laguerre-Gaussian beams (LG) with azimuthal quantum number  $\ell$  and angular momentum  $\ell\hbar$  per photon [23]:

$$\mathbf{E}_{(f,b)}(z, r, \theta, t) \sim \frac{\mathbf{E}_{(f,b)} \exp[i(-\omega_{(f,b)}t \pm k_{(f,b)}z) \pm i\ell\theta]}{(1 + iz/(k_{(f,b)}D_0^2))^2} (r/D_0)^{|\ell|} \exp\left[-\frac{r^2}{D_0^2(1 + iz/(k_{(f,b)}D_0^2))}\right], \quad (4)$$

the interference pattern is different for LG reflected from conventional mirror and phase conjugating mirror. Backward reflection from conventional spherical mirror changes the topological charge of the LG [16], exactly

in the same way as circular polarization of light changes from left to right and vice-versa in reflection [22]. In addition the intensity  $I_{tor}(z, r, \theta, t)$  vanishes on the beam axis thus an interference pattern transforms into the sequence of the equidistant rotationally invariant *toroids* separated by  $\lambda/2$  interval:

$$I_{tor}(z, r, \theta, t) = \epsilon_0 c \frac{2|\mathbf{E}_{(f,b)}|^2 2^{(\ell+1)}}{\pi \ell! D_0^2} \times [1 + \cos[(\omega_f - \omega_b)t - (k_f + k_b)z]] \times (r/D_0)^{2|\ell|} \exp\left[-\frac{2r^2}{D_0^2(1 + z^2/(k_{(f,b)}^2 D_0^4))}\right]. \quad (5)$$

On the other hand the reflection from phase-conjugating mirror (PCM) [16, 24] does not change the topological charge of LG. As a result the expression for the interference pattern is slightly different:

$$I_{tw}(z, r, \theta, t) = \epsilon_0 c \frac{2|\mathbf{E}_{(f,b)}|^2 2^{(\ell+1)}}{\pi \ell! D_0^2} \times [1 + \cos[(\omega_f - \omega_b)t - (k_f + k_b)z + 2\ell\theta]] \times (r/D_0)^{2|\ell|} \exp\left[-\frac{2r^2}{D_0^2(1 + z^2/(k_{(f,b)}^2 D_0^4))}\right]. \quad (6)$$

The intensity also vanishes at LG axis  $z$  as  $r^{2|\ell|}$ , while a self-similar argument

$$\chi = [(\omega_f - \omega_b)t - (k_f + k_b)z + 2\ell\theta], \quad (7)$$

where the azimuthal term  $2\ell\theta$  appears due to phase conjugation  $\mathbf{E}_b \sim \mathbf{E}_f^*$ , keeps the maxima of intensity at the two collocated helices each having  $\lambda$ -pitch separated from each other by  $\lambda/2$  interval (fig. 1). Thus we have the following strict correspondence between the *roll* interference pattern (3) and the helical interference pattern (6): the frequency difference  $\delta\omega = \omega_f - \omega_b$  is the cause of the translation of *rolls* with *group* velocity  $V_z = (\omega_f - \omega_b)/(k_f + k_b)$  of the wavetrain, produced by a sum of the two counter-propagating beams  $(\mathbf{E}_f + \mathbf{E}_b)$  [3]. The  $\delta\omega$  is responsible for the rotation of *helices* with angular velocity  $\delta\omega = \omega_f - \omega_b$  as well. The rotation is the cause of the *pitch* of helical interference maxima along  $z$ -axis. Consequently there exists a perfect mechanical analogy between the *solid body* rotation of the helix described by formula (6) and an Archimedean screw. Namely the positive  $\delta\omega$  corresponds to the counter-clockwise rotation and this provides the *pitch* in positive  $z$  direction for *right* helices. On the other hand the negative  $\delta\omega$  means clockwise rotation. In this case ( $\delta\omega < 0$ ) the positive translation speed in  $z$  direction takes place for the *left*-handed helices. Evidently the change of the topological charge  $\ell$  changes the direction of helix translation  $\vec{V}_z$  due to alternation of the helix hand to the opposite one for fixed  $\delta\omega$ .

This mechanical analogy is useful for the analysis of the cold atoms motion in the helical trap. Virtually the velocity vector of the condensate fragment trapped and

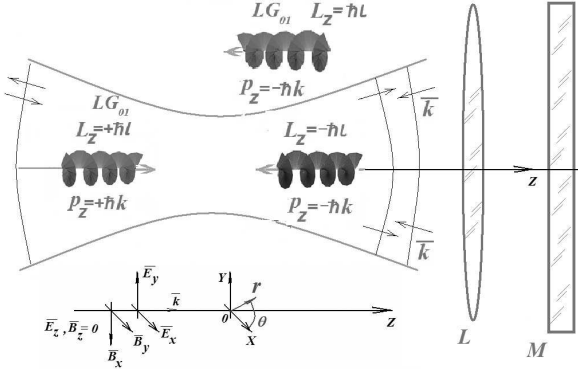


FIG. 2: Towards calculation of momentum and angular momentum of a composite wavetrain in a helical optical dipole trap (8,9). The wavetrain (upper helix) reflected from conventional mirror ( $M$ ) has opposite *hand* compared to the incident (left) helix. Thus its angular momentum  $L_z$  has positive projection  $\hbar l$  on propagation axis  $z$ . On the contrary the phase-conjugated wavetrain  $LG_{01}$  (bottom helix) has the same *hand* as the incident one. As a result the OAM of PC LG has the overturned projection  $-\hbar l$  upon propagation axis.  $L$  is a wavefront matching parabolic lens.

perfectly collocated with intensity maxima has two components  $\vec{V} = \vec{V}_z + \vec{V}_\theta$  (fig. 1). The axial component is a *group* velocity  $|\vec{V}_z| = (\omega_f - \omega_b)/(k_f + k_b)$  of the wavetrain, while the azimuthal component  $|\vec{V}_\theta| = (\omega_f - \omega_b) \cdot R$  is of kinematic nature. Such a *solid body* field of velocities is reminiscent to the rotation of a *classical* liquid together with rotating container [25] where the angular velocity  $\delta\omega(r)$  is the  $r$ -independent constant. Noteworthy the *effective* field of velocities  $\vec{V} = \hbar\nabla\theta/m$  of the optical LG vortex (4) is of different nature and this effective velocity field is equivalent to those of quantum liquid composed of particles of mass  $m$  which have orbital angular momentum  $L_z = mV_\theta r = \hbar l$  independent of  $r$  [25]. As is well known the velocity  $\vec{V} = \hbar\nabla\theta/m$ ,  $V_\theta(r) \sim r^{-1}$  and the angular velocity  $\omega(r) \sim r^{-2}$  fields of the vortex inside quantum liquid have the point singularities at the vortex core ( $r \rightarrow 0$ ).

### III. LINEAR OPTICAL LOOP PHASE-CONJUGATION

The apparent topological difference of toroidal (5) and helicoidal (6) interference patterns is due to the mutual orientation of their orbital angular momenta. The toroidal pattern appears when colliding photons have a parallel OAM's [15] while helicoidal pattern [16] arises for antiparallel OAM's. This follows from direct calculation of OAM for the  $\ell$ 'th order LG. The OAM is the expectation value of the angular momentum operator  $\hat{L}_z = -i\hbar[\vec{r} \times \nabla] = -i\hbar\frac{\partial}{\partial\theta}$  inside the interaction volume  $V \cong \pi R^2 Z_r$ :

$$\begin{aligned} \langle L_z \rangle_{(f,b)} &= \langle \Psi_{(f,b)}^\ell | \hat{L}_z | \Psi_{(f,b)}^\ell \rangle \\ &\sim \int_V (E_{(f,b)}^+)^* (-i\hbar[\vec{r} \times \nabla] E_{(f,b)}^+) d^3\vec{r} = \\ &\int (E_{(f,b)}^+)^* (-i\hbar\frac{\partial}{\partial\theta} E_{(f,b)}^+) r dr \cdot d\theta dz \sim \ell\hbar \frac{I_{(f,b)} V}{\hbar\omega_{(f,b)} c}, \end{aligned} \quad (8)$$

where  $I_{(f,b)} = \epsilon_0 c |\mathbf{E}_{(f,b)}|^2$  is the light intensity,  $\Psi_{(f,b)}^\ell = \sqrt{2\epsilon_0} E_{(f,b)}^+(z, r, \theta, t)$  is the macroscopic wavefunction of a single light photon inside a forward ( $f$ ) or backward ( $b$ ) LG wavetrains (4) with the winding number  $\ell$ . The retroreflector is placed apart from the interaction volume  $V$  located near  $z = 0$  plane within Rayleigh range  $Z_r < k_{(f,b)} D_0^2$  and the fields  $E_{(f,b)}^+$  are both calculated inside this volume (fig.2). The square modulus  $|\Psi_{(f,b)}^\ell|^2$  is a probability density for energy rather than for a particle (photon) location. This is a Sipe's single-photon wavefunction [26] which is proportional to the positive frequency component  $E_{f,b}^+$  of the counter-propagating fields. The usage of the nonrelativistic operators of the linear momentum ( $\hat{p} = -i\hbar\nabla$ ) and angular momentum ( $\hat{L}_z = -i\hbar\frac{\partial}{\partial\theta}$ ) is justified by the applicability of the paraxial approximation to the slowly diverging LG beams. In this particular paraxial case the spin-orbit coupling [27] may be neglected and the angular momentum of the photon is exactly decoupled to the spin and the orbital component:  $\hat{J} = \hat{S} + \hat{L}$ . The linear momentum expectation values  $\langle \vec{p} \rangle_{(f,b)}$  for the forward and backward LG's respectively are obtained in following way:

$$\begin{aligned} \langle p_z \rangle_{(f,b)} &= \langle \Psi_\ell | \hat{P} | \Psi_\ell \rangle \\ &\sim \int (E_{(f,b)}^+)^* (-i\hbar\nabla E_{(f,b)}^+) d^3\vec{r} = \\ &\int (E_{(f,b)}^+)^* (-i\hbar\frac{\partial}{\partial z} E_{(f,b)}^+) d^3\vec{r} \hbar k_{(f,b)} \frac{I_{(f,b)} V}{\hbar\omega_{(f,b)} c} \\ &\cong \pm N \hbar k_z, \end{aligned} \quad (9)$$

From Maxwell equations it follows that the expression for the classical momentum density of electromagnetic field is the *polar* vector  $\vec{P}$ , while angular momentum density  $\vec{M}$  is the *axial* vector [28]:

$$\vec{P}(z, r, \theta, t) = \epsilon_0 [\vec{E} \times \vec{B}]; \quad \vec{M}(z, r, \theta, t) = \epsilon_0 [\vec{r} \times [\vec{E} \times \vec{B}]] \quad (10)$$

By Ehrenfest theorem one might expect the identity of the classical and quantum mechanical calculations of the linear and angular momenta. The integration over LG interaction volume  $V$  containing cold atomic cloud gives the classical momentum  $P_z$  of the incident and reflected LG's projected on  $z$ -axis:

$$\begin{aligned} P_{z(f,b)} &\cong \frac{\epsilon_0}{c} \int_0^{2\pi} d\theta \int_0^R r dr \int_{-Z_r}^{Z_r} [\vec{E} \times \vec{B}] dz \Big|_z \\ &\cong \pm I_{(f,b)} \cdot \pi R^2 \cdot Z_r / c^2, \end{aligned} \quad (11)$$

where  $2Z_r$  is length of trapped cloud,  $R = D_0/2$  is the radius of helix. In a same way the classical angular momenta  $L_z$  of LG beams inside the interaction volume  $V \cong 2\pi R^2 Z_r$  projected on  $z$ -axis are as follows:

$$L_{z(f,b)} = \epsilon_0 \int_0^{2\pi} d\theta \int_0^R r dr \int_{-Z_r}^{Z_r} [\vec{r} \times [\vec{E} \times \vec{B}]] dz \Big|_z \\ \cong \pm \ell \cdot I_{(f,b)} \cdot \pi R^2 \cdot Z_r / (c \omega_{(f,b)}). \quad (12)$$

The ratio of the angular and linear momenta proved to be equal to  $L_z/P_z \sim \ell c/\omega_{(f,b)}$  [28]. Consequently both classically and quantum mechanically when linearly polarized LG-beam (with  $\vec{S} = 0$ ) is retroreflected from conventional mirror, the *polar* vector of the optical momentum  $\vec{P}$  changes direction to the opposite one while the *axial* vector of the angular momentum  $\vec{J} = \vec{L}$  remains unchanged due to the isotropy of reflector [16]. Thus the topological charge  $\ell$  in (4) alters sign. The next reflection will change the topological charge once again due to the same reasons. From this follows that after an *even* number of reflections the topological charge will be conserved. Because LG is the eigenfunction of a free space parabolic wave equation it's propagation is self-similar in free space. The same holds for the passage through the smooth curved optical surfaces alike thin quasiparabolic lenses. In addition the LG's reflection from planar or smooth curved surfaces is self-similar too. Consequently the linear momentum and angular momentum conserve their mutual orientation (projection of angular momentum upon propagation axis, or momentum [29]) after the *even* number of reflections from isotropic optical elements.

In contrast to the conventional mirrors the wavefront reversing (PC) mirrors are essentially anisotropic optical elements [16, 18]. Due to the internal helical structures, e.g. acoustical vortices in SBS mirrors, the PC mirror overturns the angular momentum of the incident beam. Thus because the linear momentum  $\vec{P}$  is overturned too, the mutual orientation of  $\vec{P}$  and  $\vec{L}$  is conserved and the topological charge  $\ell$  is not changed by an *ideal* PC mirror.

For the linear polarization, i.e. for zero-spin LG-photons with winding number  $\ell$ , the equivalence between *nonlinear* PC-mirrors, like Stimulated Brillouin mirrors, photorefractive mirrors, liquid crystal light valves etc. and topologically equivalent set of a *linear* optical elements may be achieved in a closed *loop* setup. The simplest conceivable configuration composed of plane mirrors, wavefront curvature compensating lenses and beam-splitters is shown at fig.3. The goal of proposed setup is to counter-direct the splitted LG beams. The four reflections look as a necessary minimum, because the incidence angles much above 45 degrees will enhance the effects of LG transformation and a small sliding of a beam along the reflecting surface [30] caused by unavoidable anisotropy of the mirror tilted with respect to the LG propagation axis. The auxiliary physical restrictions on this *loop* setup are in maintaining the path difference  $\Delta L$  of splitted LG's to be smaller than coherence length of

trapping laser field ( $\Delta L \ll c \cdot \tau_{coh}$ ) inside the helical interference volume (the latter is located inside vacuum tube with cold atoms, see fig.3). The parabolic wavefront curvature due to the free-space propagation beam spread is to be compensated by parabolic (sufficiently thin) lenses.

These restrictions upon coherence length, wavefront curvature and small frequency shift  $\delta\omega$  were already implemented successfully in experimental setups for trapping the cold atoms in a standing, moving and accelerating optical gratings [3]. Thus a *linear* optical loop setup outlined above provided the *even* number of reflections per a single loop roundtrip might be a practical equivalent of the nonlinear optical PC retroreflector [16, 19].

Because of the Earth rotation having angular frequency  $\Theta_{\oplus}$  and the optical table one  $\Omega_{iab}$  the *Sagnac loop* phase shift to occur [21]:

$$\delta\vartheta = \frac{8\pi A \Omega_r}{c \cdot \lambda}, \quad (13)$$

where  $\Omega_r = \Theta_{\oplus} + \Omega_{iab}$  is angular speed of rotation of the laboratory frame,  $P$ ,  $A$  are the perimeter and the square of the loop respectively. This additional phase shift  $\delta\vartheta$  appears in the self-similar variable [21]:

$$\chi = [(k_f + k_b)z + 2\ell\theta + \delta\vartheta], \quad (14)$$

resulting in the static phase shift in the interference pattern (6). The small frequency shift which might be induced by a frequency ramp [3]  $\delta\omega = \omega_f - \omega_b \approx 2\pi 10^{-(1-3)} rad/sec$  or due to angular Doppler shift [31] is required to cause the helix rotation [16]. Moreover there exists the possibility of obtaining the detuning  $\delta\omega$  of the counter-propagating optical due to Sagnac effect in the optical *loop* with laser gain medium inside [21]:

$$\delta\omega = \frac{16\pi^2 A \Omega_r}{P \cdot \lambda}. \quad (15)$$

From the above it follows that rotation of the *passive* loop will cause the static *pitch* of helical pattern, proportional to  $\Omega_r$ . On the other hand, rotation  $\Omega_r$  of the *active* loop with an optical amplifier inside results in the slow rotation of the helical pattern with angular frequency  $\delta\omega$ .

#### IV. MACROSCOPIC WAVEFUNCTIONS FOR A COLD BOSONS IN A RED-DETUNED HELICAL TRAPS.

Consider an ultracold bosonic cloud loaded in a helical interference pattern (6). The current state of art experiments are performed with a atomic ensemble loaded in elongated trap [3] and released afterwards. Next a periodic optical potential is applied to study the Bloch oscillations, macroscopic Landau-Zener tunneling and Josephson effects [2, 4]. In our case the optical potential have the following form:

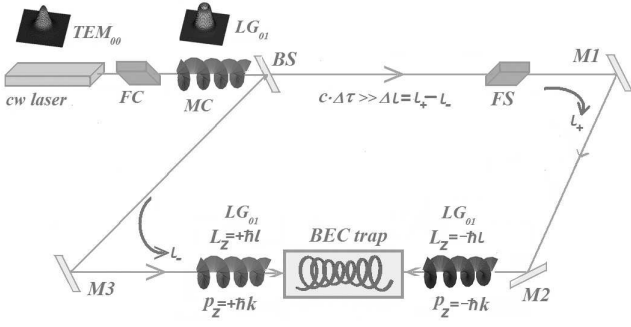


FIG. 3: The closed loop setup for producing the helical interference pattern. The CW laser emits fundamental mode which passes through Faraday isolator (FC). The mode-converter MC made of the two cylindrical lenses [28] transforms the fundamental Gaussian mode into LG beam with topological charge  $\ell$ . The beamsplitter BS changes the topological charge of the reflected beam to the opposite one and leaves the  $\ell$  unchanged for transmitted LG. After the even number of reflections both LG beams meet inside trap volume  $V$ . The path difference  $\Delta L = l_+ - l_-$  is assumed to be smaller than coherence length  $L_{coh} = c \cdot \tau$ , where  $\tau$  is the coherence time. The minimal amount of reflections for the in-plane geometry is required for turnover of the angular momentum  $L_z$  to the opposite one is equal 2. The clockwise beam  $l_+$  experiences two reflections at mirrors M1 and M2 after the passage through BS, the counterclockwise beam  $l_-$  after reflection from BS changes its OAM (and topological charge  $\ell$ ) once again at mirror M3. As a result both LG possess the opposite angular momenta ( $\hbar$  per photon) and produce helical interference pattern in trapping volume. The parabolic wavefront correcting elements are not shown. The frequency shifting FS box denotes symbolically the detuning of the counter-propagating beams  $\delta\omega$  caused by rotation  $\Omega_r$  or frequency ramp. For active loop FS designates the laser amplifier placed inside loop [21].

$$V_{opt}(z, r, \theta, t) = -\frac{Re[\alpha(\omega)]}{2\epsilon_0 c} I_{tw}(z, r, \theta, t),$$

$$\alpha(\omega) = 6\pi\epsilon_0 c^3 \frac{\Gamma/\omega_0^2}{(\omega_0^2 - \omega^2 - i(\omega^3/\omega_0^2)\Gamma)}, \quad (16)$$

where  $\alpha(\omega)$  is the polarizability of atom, which is real, i.e.  $\alpha(\omega) \approx Re[\alpha]$  at large detunings from resonance  $\omega - \omega_0$ ,  $\Gamma$  is atomic linewidth,  $\epsilon_0$  is the dielectric constant of vacuum [1, 13]. For a low temperatures ( $T \cong 0$ ), red detuning  $\omega_0 - \omega_{f,b} > 0$  and when a number of trapped bosons  $N = \int |\Psi|^2 d^3\vec{r}$  is large enough, the Gross-Pitaevskii equation (GPE) for the macroscopic BEC wavefunction  $\Psi$  confined by the helical potential  $V_{opt}$  reads:

$$i\hbar \frac{\partial \Psi(\vec{r}, t)}{\partial t} = \hat{H}\Psi(\vec{r}, t) = -\frac{\hbar^2}{2m} \Delta \Psi + V_{opt}(z, r, \theta, t) \Psi + \frac{4\pi\hbar^2 a_s(\vec{B})}{m} |\Psi|^2 \Psi, \quad (17)$$

where  $a_s(\vec{B}) = a_{bg}(1 + \Delta_B/(B - B_F))$  is magnetic field-dependent  $s$ -wave scattering length,  $a_{bg}$  is background

value of  $a_s$ ,  $B_F$  and  $\Delta_B$  are the Feshbach magnetic induction and resonance width respectively. For the sufficiently numerous ultracold atomic ensemble ( $N \cong 10^5$ ) the quantum pressure term following from uncertainty principle is negligible ( $\hbar^2 \Delta \Psi / 2m \sim 0$ ) compared to the optical trapping and interaction terms. Hence one might expect that a Thomas-Fermi approximation (TFA) is valid when interaction is repulsive, i.e. for the positive  $a_s$  [20]. The estimates will be done for simplicity in the vicinity of the LG-beam waist, i.e. within Rayleigh range, when  $z \ll k_{f,b} D_0^2$ . In this region the following TFA wavefunction satisfies GPE (17):

$$\Psi_{fun}(z, r, \theta, t) \approx \Phi(r) \exp\left[-\frac{i\mu(r)t}{\hbar} + i\Phi(r)^2 \sin(\delta\omega t - 2k_z z + 2\ell\theta)\right], \quad (18)$$

where  $\mu(r)$  is a local ( $r$ -dependent) value of chemical potential defined as:

$$\mu(r) = 4\pi\hbar^2 a_s \Phi(r)^2 / m;$$

$$\Phi(r)^2 = \exp(-2r^2/D_0^2) \cdot (r/D_0)^{2|\ell|} \cdot \frac{\alpha(\omega) I_0}{2\epsilon_0 c \cdot \hbar \cdot \delta\omega};$$

$$I_0 = 2\epsilon_0 c |\mathbf{E}_{(f,b)}|^2 \quad (19)$$

The wavefunction (18) is normalizable and fits GPE by direct substitution. In particular the TFA density of atoms  $\rho_{fun}(z, r, \theta, t) = |\Psi_{fun}|^2 = \Phi(r)^2 \sim \exp(-2(r/D_0)^2)/(r/D_0)^{2|\ell|}$  is  $(z, t)$ -independent "funnel" collocated with the optical helix  $I_{tw}(z, r, \theta, t)$ . The phase modulation of  $\Psi$  is maximal near the density maximum  $\rho_{fun}(z, r, \theta, t)$  and decreases down to zero on LG axis and outside the LG waist. The phase modulation has sinusoidal dependence on azimuthal angle  $\theta$ .

The other solution in TF approximation might be obtained for  $r$ -independent chemical potential  $\mu = const$ . In this regime the mean field wavefunction  $\Psi$  is a sum of the two phase-conjugated wavefunctions with the opposite topological charges  $\ell$ :

$$\Psi_{helix}(z, r, \theta, t) = \Psi_\ell(z, r, \theta, t) + \Psi_{-\ell}(z, r, \theta, t) \cong \Psi_{\pm\ell}(z=0) \cdot (r/D_0)^{|\ell|} \exp\left[-\frac{r^2}{D_0^2(1+iz/(k_{(f,b)}D_0^2))}\right] \left\{ \frac{\exp[-i\mu_f t/\hbar + ik_f z + \ell\theta]}{(1+iz/(k_f D_0^2))^2} + \frac{\exp[-i\mu_b t/\hbar - ik_b z - \ell\theta]}{(1+iz/(k_b D_0^2))^2} \right\}, \quad (20)$$

where the difference of the partial chemical potentials  $(\mu_f - \mu_b)$ , associated with the each of "counter-propagating" wavefunctions  $\Psi_\ell, \Psi_{-\ell}$  is adjusted to the frequency difference of counter-propagating optical fields  $(\mu_f - \mu_b)/\hbar = \delta\omega = \omega_f - \omega_b$ . The substitution of this TFA wavefunction into GPE gives the following link for parameters:

$$\rho_{helix}(z, r, \theta, t) = |\Psi_{helix}(z, r, \theta, t)|^2 = \frac{\mu - \alpha(\omega) I_{tw}(z, r, \theta, t)/2\epsilon_0 c}{g}, \quad (21)$$

where  $\mu = \mu_f - \mu_b$  is a constant ( $z, r, \theta, t$ -independent) value of chemical potential,  $g = 4\pi\hbar^2 a_s(\vec{B})/m$  is the interaction parameter. This equation means the quasichlassical restriction imposed on a homogeneity of chemical potential of the system in an external field  $V_{opt}$  [20]:

$$\mu_1[\rho_{helix}(z, r, \theta, t)] + \alpha(\omega)I_{tw}(z, r, \theta, t)/2\epsilon_0 c = \mu = const \quad (22)$$

obtained for the gas with the local value of chemical potential  $\mu_1(\rho(\vec{r}, t)) = g\rho_{helix}$ . In accordance to this solution the density of the cold atomic ensemble  $\rho(z, r, \theta, t)$  is a perfectly correlated with the rotating optical helix potential  $I_{tw}(z, r, \theta, t)$  as depicted at fig.1:

$$\begin{aligned} \mu - \frac{\alpha(\omega)I_{tw}(z=0) \cdot [1 + \cos(\delta\omega t + 2kz \pm 2\ell\theta)]/2\epsilon_0 c}{g(1 + z^2/(k^2 D_0^4))} \times \\ \times (r/D_0)^{2|\ell|} \exp \left[ - \frac{2r^2}{D_0^2(1 + z^2/(k_{(f,b)}^2 D_0^4))} \right], \end{aligned} \quad (23)$$

where  $k = k_f \cong k_b$ , The density of ultracold ensemble  $\rho_{helix}$  rotates as a "solid body" with a pitch of the  $\lambda/2$ . The speed of the axial translation is  $V_z = \lambda\delta\omega/4\pi$ .

## V. CONCLUSION

In this paper we demonstrated the procedure of getting exact expressions for the macroscopic wave functions of the sufficiently large ultracold atomic ensemble

$N \cong 10^5$  trapped by a slowly rotating helical optical potential. The solutions of the Gross-Pitaevsky equation were obtained in the Thomas-Fermi approximation. The conventional solution  $\Psi_{helix}(z, r, \theta, t)$  with homogeneous chemical potential  $\mu$  is perfectly correlated with the optical intensity  $I_{tw}(z, r, \theta, t)$  and rotates with the frequency difference of the bichromatic interference pattern  $\delta\omega$ . The solution with spatially varying chemical potential  $\mu(r)$  (19) has a stationary in time isodensity profile  $\rho_{fun}(z, r, \theta, t)$ , looking like "funnel" whose maximum is collocated with average radius of LG beam pattern. In this particular regime the rotation is hidden and embedded in phase of  $\Psi_{fun}$ .

The possible experimental implementation of helical trapping might be the sudden switching of the helical potential after condensate release from elongated optical trap in a way similar to switching of accelerated grating in [3]. The solution with rotating helical density profile  $\rho_{helix}(z, r, \theta, t)$  (20) describes the condensate dragging by optical potential analogously to NIST rotating lattice tests [7]. Another solution (18) with nonrotating density profile  $\rho_{fun}(z, r, \theta, t)$  demonstrates the seemingly absence of dragging, but helical phase field means the nonzero curl of velocity  $\vec{V} = \hbar\nabla\theta/m$ .

The red detuned rotating helical optical trap might be arranged with conventional optical elements, namely beam splitters, low curvature mirrors, spherical and cylindrical lenses. The proposed *loop* trapping geometry offers a possibility of the not only rotation detection but assembling of the cold protein-like molecules as well.

The partial support of the Russian fund for Basic Research Grant 08-02-01229 is acknowledged.

- 
- [1] R.Grimm, M.Weidemuller and Yu.B.Ovchinnikov, Adv.At.Mol.Opt.Phys. **42**, 95 (2000).
  - [2] O.Morsch, M.Oberthaler, Rev.Mod.Phys. **78**, 179 (2006).
  - [3] M. Cristiani, O. Morsch, J. H. Muller, D. Ciampini, and E. Arimondo, Phys.Rev.A, **65**, 063612 (2002).
  - [4] S.Giorgini, L.P.Pitaevskii, S.Stringari, Rev.Mod.Phys. **80**, 1215 (2008).
  - [5] I.Bloch, J.Dalibard, W.Zwenger, Rev.Mod.Phys. **80**, 885 (2008).
  - [6] B.Damski, H.Fehrmann, H.H.Everts, M.Baranov, L.Santos and M.Lewenstein, Phys.Rev.A**72**, 053612 (2005).
  - [7] S.Tung, V.Schweikhard, and E.A.Cornell, Phys.Rev.Lett., **97**, 240402 (2006).
  - [8] E.R.I.Abraham, J.Tempere and J.T.Devreese, Phys.Rev, **64A**, 023603 (2002).
  - [9] William T M Irvine 2010 Linked and knotted beams of light, conservation of helicity and the flow of null electromagnetic fields *J. Phys. A: Math. Theor.* **43**, 385203.
  - [10] A.Yu.Okulov, Phys.Rev.A , **80**, 013837 (2009).
  - [11] Y.F.Chen, Y.P.Lan, Phys.Rev.A, **64**, 063807 (2001).
  - [12] K.Staliunas, C.O.Weiss, *JOSA B* **12**, 1142 (1995).
  - [13] A.Yu.Okulov, J.Mod.Opt., **55** , 241-257 (2008).
  - [14] A.Yu.Okulov, Laser Physics, **17**, 1796 (2009).
  - [15] T. Puppe, I. Schuster, A. Grothe, A. Kubanek, K. Murr, P.W.H. Pinkse, and G. Rempe, Phys.Rev.Lett., **99**, 013002 (2007).
  - [16] A.Yu.Okulov, J.Phys.B., **41**, 101001 (2008).
  - [17] M.Bhattacharya, Opt.Comm. **279**, 219 (2007).
  - [18] A.Yu.Okulov, JETP Lett., **88**, 631 (2008).
  - [19] M.Woerdemann, C.Alpmann and C.Denz, Opt. Express, **17**, 22791(2009).
  - [20] F. Dalfovo, S.Giorgini, S.Stringari, L.P.Pitaevskii, Rev.Mod.Phys.**71**,463(1999).
  - [21] M.O.Scully, M.S.Zubairy, "Quantum optics", Ch.17, (Cambridge University Press) (1997).
  - [22] B.Y.Zeldovich, N.F.Pilipetsky and V.V.Shkunov "Principles of Phase Conjugation",Ch.2 (Berlin:Springer-Verlag )(1985).
  - [23] J.Leach,M.J.Padgett,S.M.Barnett,S.Franke-Arnold, and J.Courtial, Phys.Rev.Lett., **88**, 257901 (2002).
  - [24] A.V.Mamaev, M.Saffman and A.A.Zozulya, Phys.Rev.A, **56**, R1713 (1997).
  - [25] R.P.Feynman, "Statistical mechanics", (Ch.11, Reading, Massachusetts,1972).
  - [26] J.E.Sipe, Phys.Rev.A, **52**, 1875 (1995).
  - [27] V.S.Liberman and B.Y.Zeldovich, Phys.Rev.A, **46**, 5199 (1992).

- [28] L.Allen, M.W.Beijersbergen, R.J.C.Spreuw and J.P.Woerdman, Phys.Rev.A, **45**, 8185-8189 (1992).
- [29] E.M.Lifshitz, L.P.Pitaevskii and V.B.Berestetskii, "*Quantum Electrodynamics*",(Landau and Lifshitz Course of Theoretical Physics, Butterworth-Heineman, Oxford) § 6,8 (1982).
- [30] K.Yu.Bliokh and Yu.P.Bliokh, Phys.Rev.Lett., **96**, 073903 (2006).
- [31] J. Arlt, M. MacDonald, L. Paterson, W. Sibbett, K. Volke-Sepulveda and K. Dholakia, Opt. Express, **10**(19),844(2002).